Supporting Information for Correlating the Formation Protocols of Solid Electrolyte Interphase with Practical Performance Metrics in Lithium Metal Batteries

Solomon T. Oyakhire[1], Wenbo Zhang[2], Zhiao Yu[3], Sarah E. Holmes[3], Philaphon Sayavong[3], Sang Cheol Kim[2], David T. Boyle[3], Mun Sek Kim[1,2], Zewen Zhang[2], Yi Cui[2,4,5*], Stacey F. Bent[1,4*]

1 Department of Chemical Engineering, Stanford University, Stanford, CA 94305, USA.

2 Department of Materials Science and Engineering, Stanford University, Stanford, CA 94305, USA.

3 Department of Chemistry, Stanford University, Stanford, CA 94305, USA.

4 Department of Energy Science and Engineering, Stanford University, Stanford, CA 94305, USA.

5 Stanford Institute for Materials and Energy Sciences, SLAC National Accelerator Laboratory, 2575 Sand Hill Road, Menlo Park, CA 94025, USA.

* Email: yicui@stanford.edu

* Email: sbent@stanford.edu

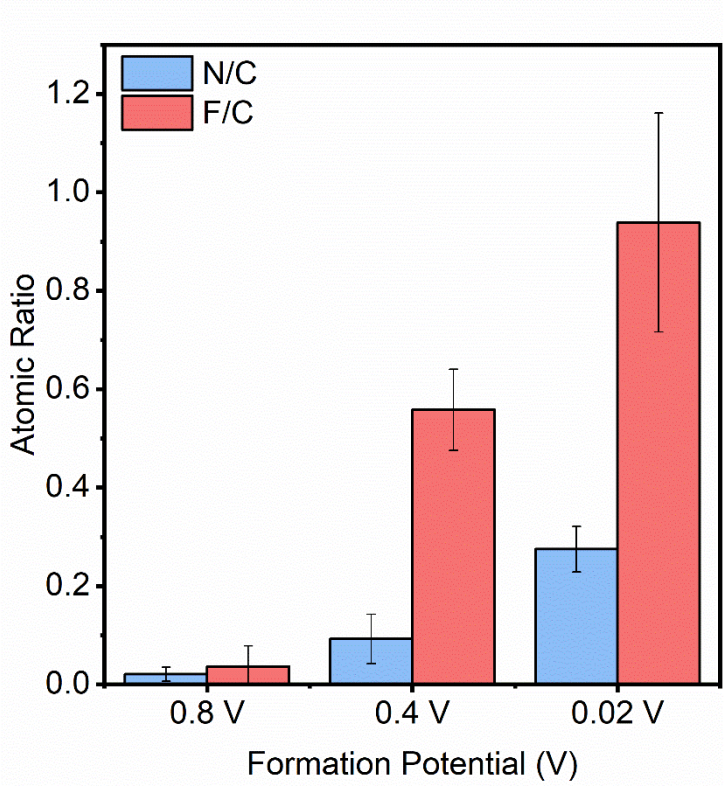

Figure S1. Average atomic ratio of N/C and F/C in SEIs formed at different voltages. The data was collected from three distinct spatial locations with the error bars representing one standard deviation from the average.

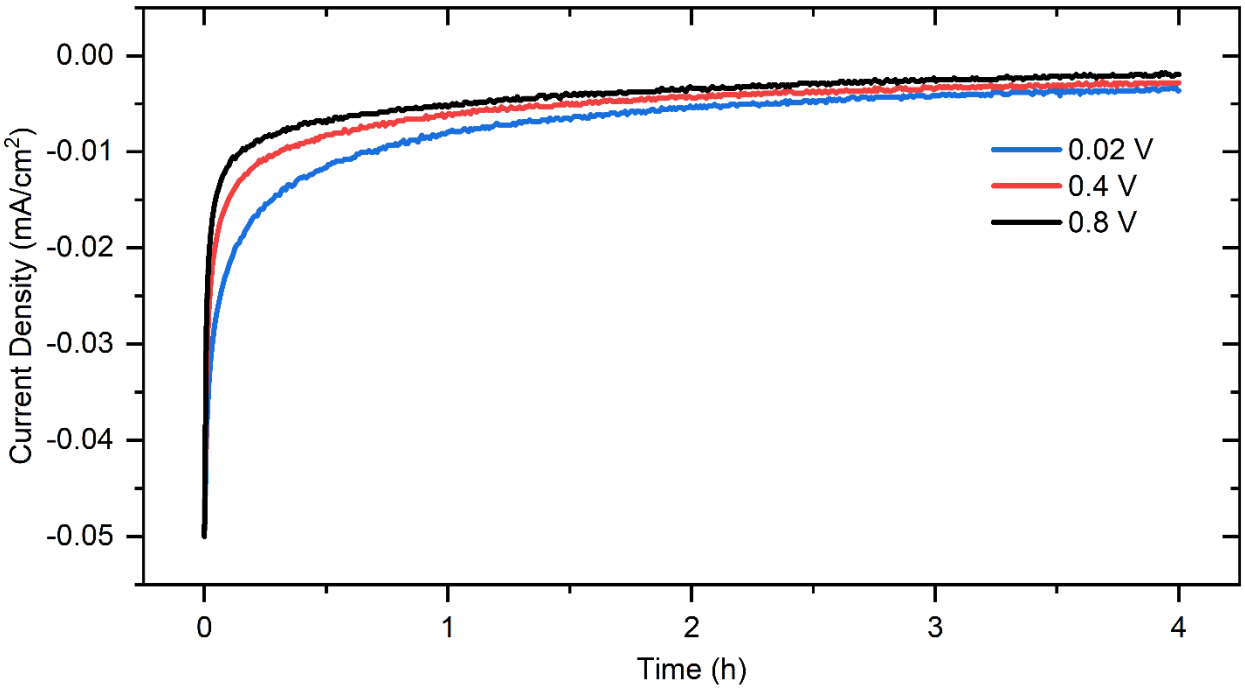

Figure S2. Current vs time trends during potential holds.

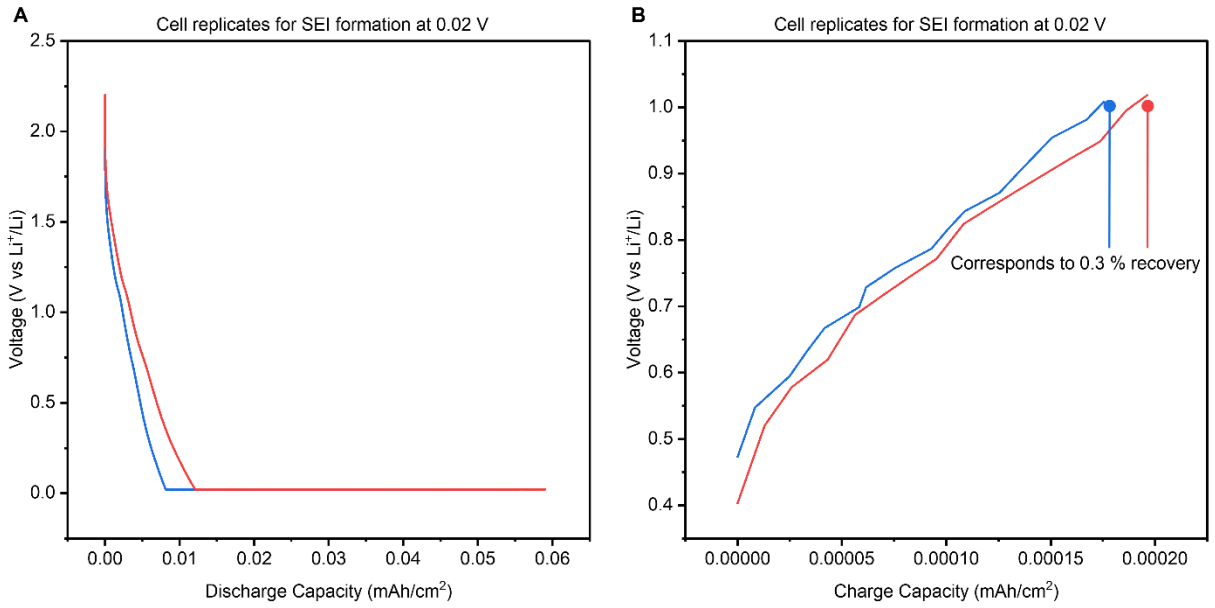

Figure S3. Quantifying SEI reversibility with coulometric methods. **A.** Voltage plotted against discharge capacity during SEI formation (constant current of -50 µA/cm^2 until 0.02 V and constant voltage for 4 hours). **B.** Voltage plotted against charge capacity during SEI oxidation under a constant current of 1 mA/cm^2.

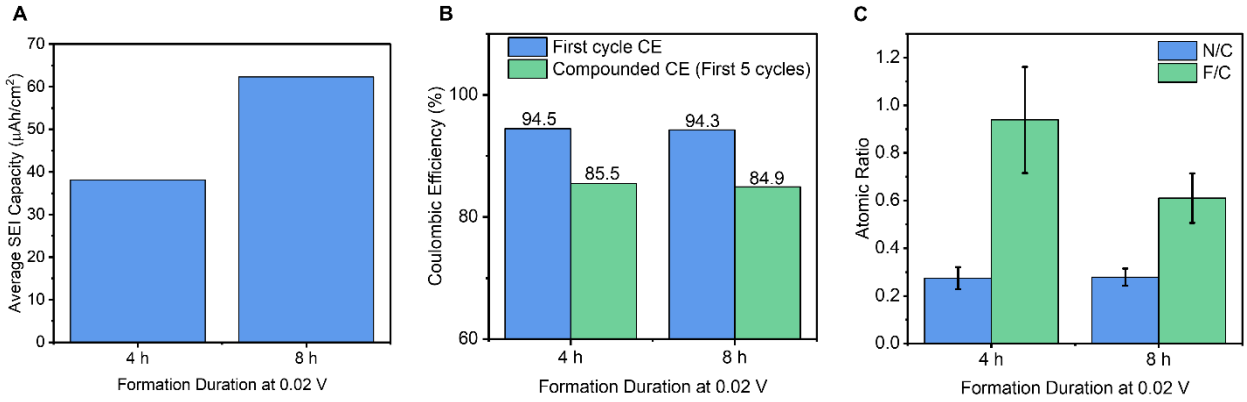

Figure S4. Decoupling the effects of SEI chemistry and SEI capacity on CE. **A.** SEI capacity as a function of formation duration at 0.02 V averaged over two cells each. **B.** Coulombic efficiency as a function of formation duration, averaged over two cells each. **C.** Atomic ratio as a function of formation duration, averaged over at least 3 distinct locations on the SEI. Measurements were carried out using the same electrolyte batch.

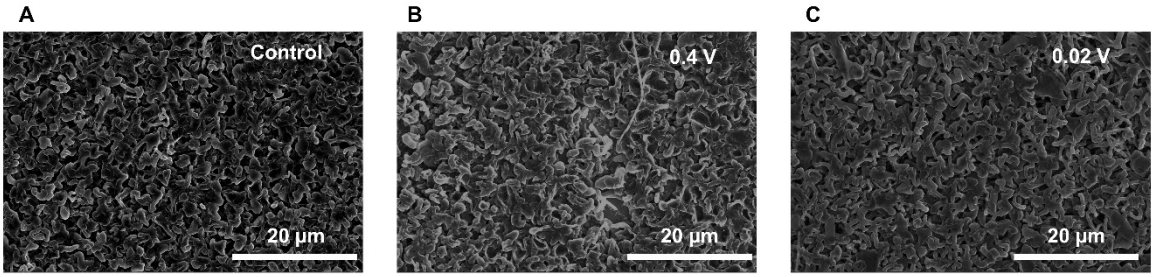

Figure S5. Morphology of lithium in the first electrochemical cycle after **A.** Control conditions, **B.** formation at 0.4 V, and **C.** formation at 0.02 V.

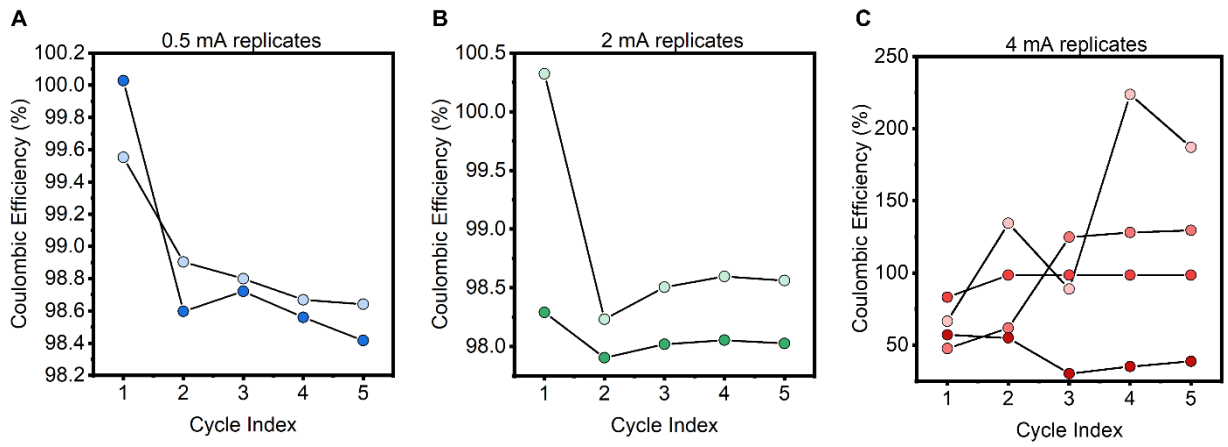

Figure S6. Short-term cycling results of Li||Cu cells cycled at 1 mA/cm^2 and 1 mAh/cm^2 after constant current SEI formation at **A.** 0.5 mA/cm^2, **B.** 2 mA/cm^2, and **C.** 4 mA/cm^2

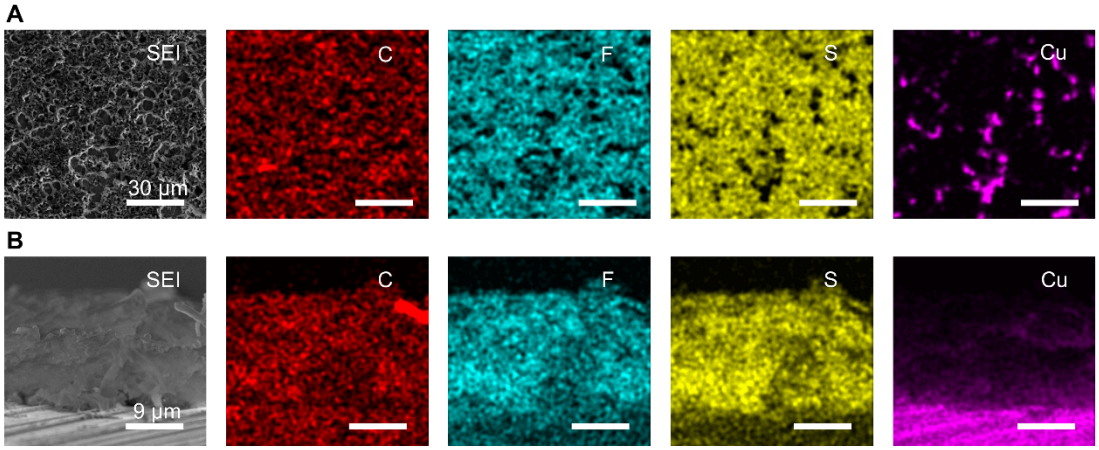

Figure S7. SEM-EDS images of the SEI formed at 0.5 mA/cm^2, displayed in the **A.** top view and **B.** side view, respectively.

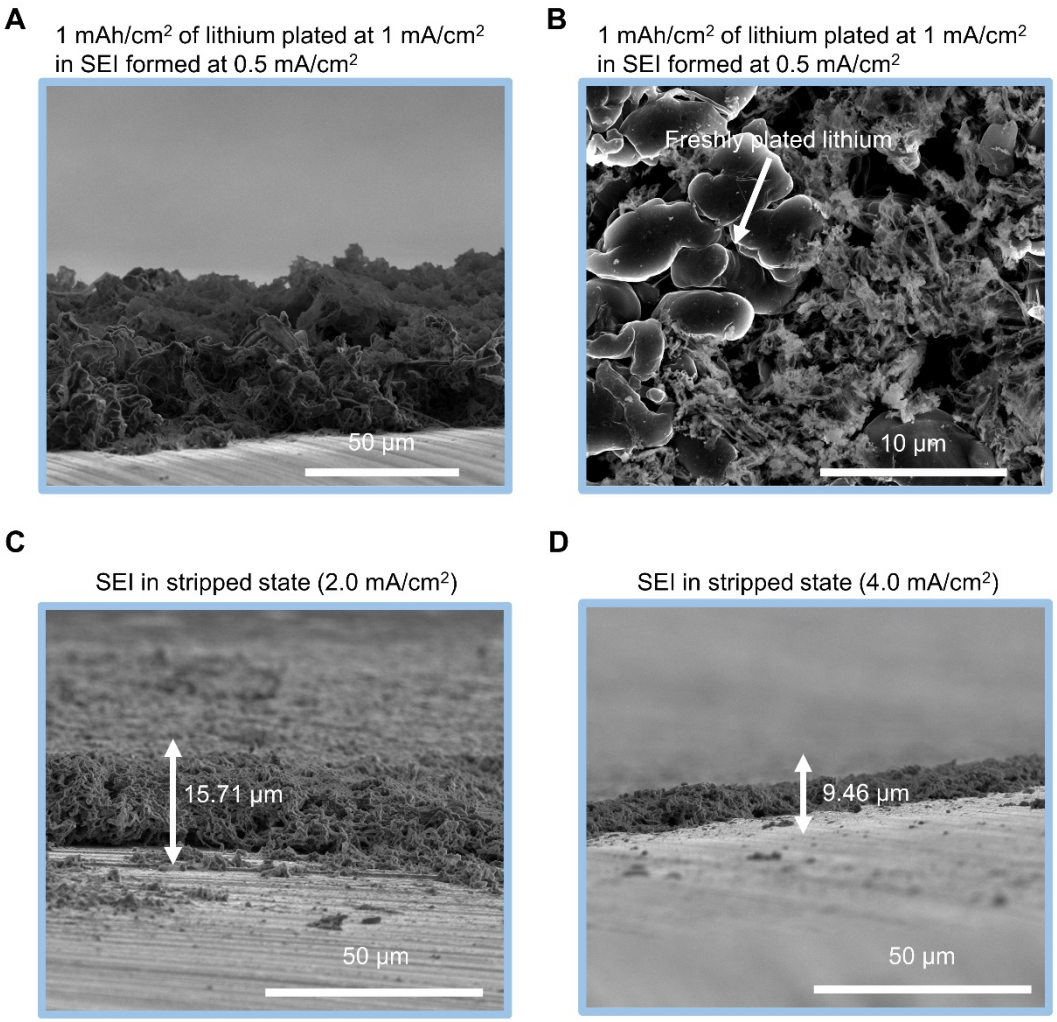

Figure S8. A, B. SEM cross-sectional and plan view, respectively of 1 mAh/cm^2 lithium plated at 1 mA/cm^2 within the 0.5 mA/cm^2 SEI structure formed in Figure 3D. **C, D.** Cross-sectional view of porous SEI formed atop copper after 10 cycles of plating and stripping 0.5 mAh/cm^2 of lithium at 2 mA/cm^2 and 4 mA/cm^2 respectively.

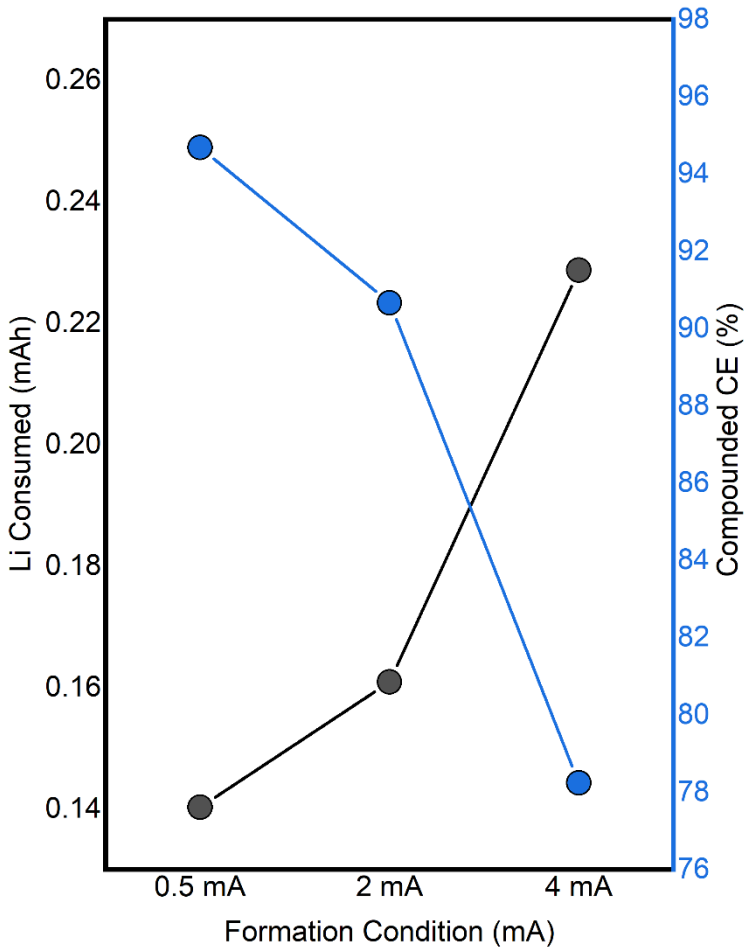

Figure S9. Lithium consumed as a function of constant current formation protocols. Reported currents are normalized to an active electrode area of 1 cm^2.

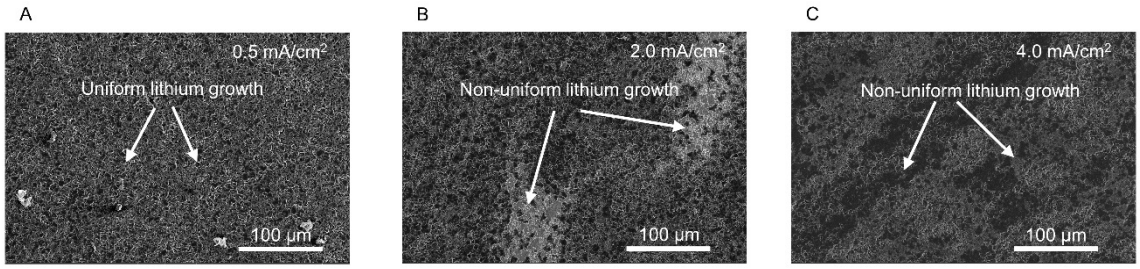

Figure S10. Lithium deposition morphology after SEI formation at **A.** 0.5 mA/cm^2 **B.** 2 mA/cm^2, and **C.** 4 mA/cm^2.

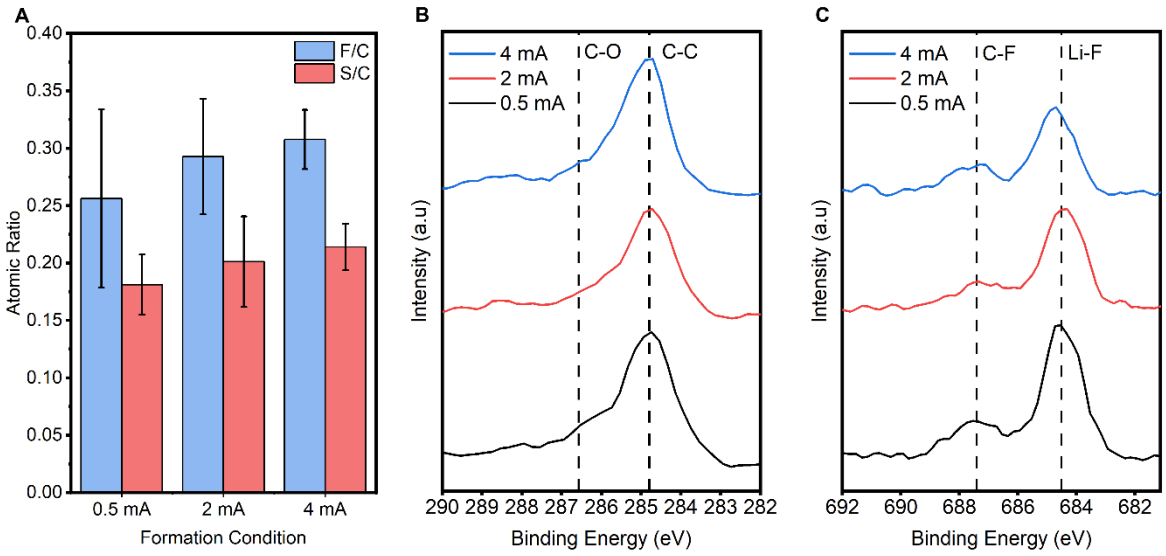

Figure S11. A. Atomic ratio of S/C and F/C collected from three distinct locations in SEIs formed at different current densities. **B, C.** XPS high resolution profile of SEIs formed at different current densities showing the C1s and F1s spectra, respectively. Reported currents are normalized to an active electrode area of 1 cm^2.

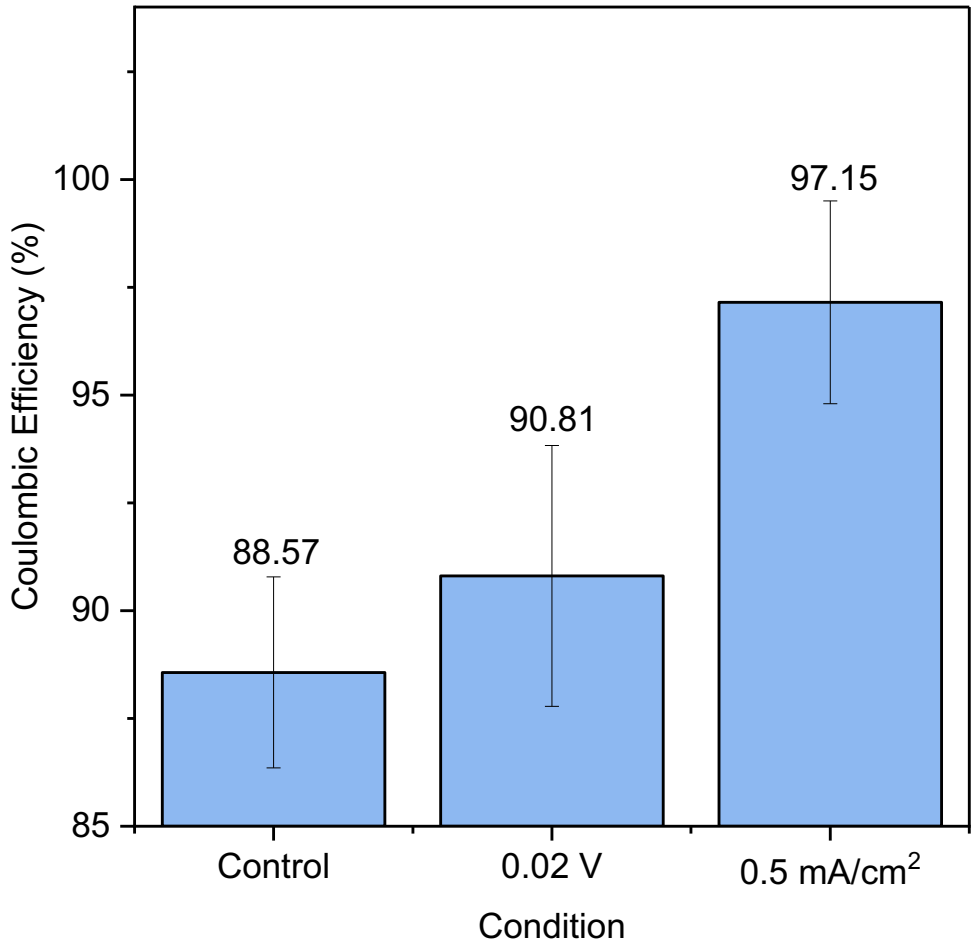

Fig S12. Average CE of Li|Cu Cells after 24 hours of aging obtained using three cells. Error bars represent one standard deviation from the average.

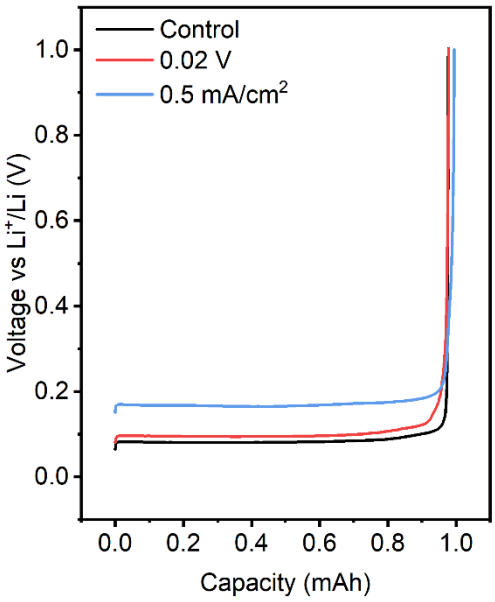

Fig S13. Voltage profiles for the unaged cells during lithium stripping at 1 mA/cm^2 after the first electrodeposition cycle at 1 mA/cm^2

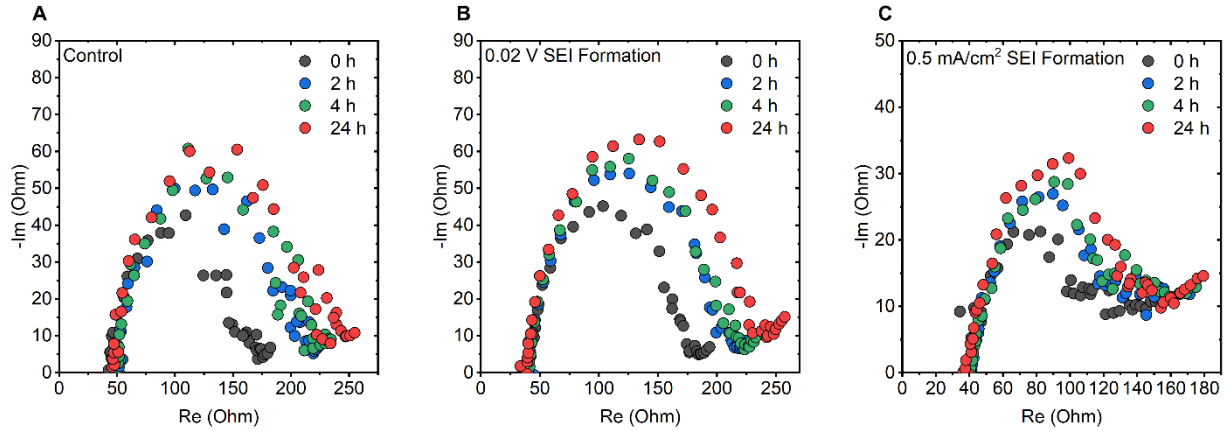

Fig S14. Nyquist plots of Li||Cu cells with lithium deposited on Cu depicting changes in interfacial resistance over a 24-hour aging period for **A.** Control, **B.** 0.02 V, and **C.** 0.5 mA/cm^2 cells, respectively.

Supplementary Note 1

The Nyquist plots for the aged cells depict the interfacial impedance of the lithium source and electrodeposited lithium. Total interfacial resistance (R_t) was extracted as the width of each semicircle, and the interfacial resistance of the electrodeposited lithium was calculated as half of the total interfacial resistance: $\frac{R_t}{2}$.